SIMILARITIES IN ZONING OF PYROXENES FROM QUE94201 AND EETA79001 MARTIAN METEORITES. T. Mikouchi[1], M. Miyamoto[1] and G. McKay[2], [1]Mineralogical Institute, Graduate School of Science, University of Tokyo, 7-3-1 Hongo, Bunkyo-ku, Tokyo 113, JAPAN, [2]Mail Code SN4, NASA Johnson Space Center, Houston, TX 77058, USA. e-mail: mikouchi@min.s.u-tokyo.ac.jp

INTRODUCTION

Complex zoning of minerals is often observed in volcanic rocks and experimental products, and is considered to be produced by crystal growth. QUE94201, a recently discovered basaltic shergottite, contains coarse-grained complexly zoned crystals of pyroxene [1, 2, 3, 4, 5]. The QUE94201 pyroxene is zoned from Mg-rich pigeonite cores through an intermediate zone of Mg-rich augite and then to extremely Fe-rich pigeonite rims. This unique zoning of pyroxene has been reported from Apollo lunar mare basalts such as 12021 [6], however, no similar zoning of pyroxene has been reported from martian meteorites. We have surveyed pyroxenes of martian meteorites, especially shergottites using an elemental mapping technique by JEOL JXA8900L electron microprobe, and found that pyroxenes from lithology B of EETA79001 (EETA79001B) show similar complex zoning to QUE94201 pyroxenes. Zoning of this type has not been detected from pyroxenes in Zagami, ALH77005, LEW88516, and Y793605. The affinity of zoning pattern and chemical composition between QUE94201 and EETA79001B pyroxenes indicate similar crystallization condition of these shergottites, although QUE94201 is more enriched in late-crystallized phases.

QUE94201 PYROXENE

The size of QUE94201 pyroxene is variable, ranging up to 2 mm long. Pyroxenes are extensively zoned from Mg-rich pigeonite core ($Mg_{62}Fe_{30}Ca_8$) through an intermediate zone of Mg-rich augite ($Mg_{44}Fe_{20}Ca_{36}$) and then to extremely Fe-rich pigeonite rims ($Mg_5Fe_{81}Ca_{14}$). Pyroxeferroite is partly present along the edge. Some pyroxenes show spectacular square-shaped augite zones (Fig. 1a and 1b), whereas some show incomplete mantling by the effect of off-center cut of the crystal. Because the zoning pattern is complicated, the zoning profiles from core to rim show different trends according to the traverse by electron microprobe [3]. The zones are parallel to {110} as indicated by their parallelism with two-sets of cleavage planes that are usually parallel to {110} in pigeonite and augite. The X-shaped bridges are observed connecting inner corners of augite zones (Fig. 1a). These directions are parallel to the *a* and *b* crystallographic axes. The twin plane of (100) is parallel to one of these directions.

EETA79001 PYROXENE

EETA79001B pyroxenes are clearly more coarse-grained than those from lithology A of EETA79001 (EETA79001A), reaching up to 3.5 mm long. Although pyroxenes in EETA79001B show different shapes on the thin section due to different cut of the crystal, it is common that the cores are Mg-rich pigeonites and they are mantled by Mg-rich augite regions (Fig. 2a and 2b). The rim is Fe-rich pigeonite. The most Mg-rich pyroxene is the core of the largest pyroxene grain, and it is $Mg_{73}Fe_{22}Ca_5$. A more typical core composition is $Mg_{64}Fe_{26}Ca_{10}$. The augite mantle is $Mg_{46}Fe_{22}Ca_{32}$, and the Fe-rich pigeonite rim reaches $Mg_9Fe_{76}Ca_{15}$. The augite zones look parallel to the elongated axis, probably *c*, and show similar geometrical growth parallel to {110} as seen in QUE94201 augite zones. The zoning pattern is complex like QUE94201 pyroxene, and EETA79001B pyroxenes also have different zoning profiles depending upon different microprobe traverses. The EETA79001B pyroxenes are typically twinned on the plane parallel to the *c* axis. Shock-induced fine lamellae are visible perpendicular to the *c* axis. Thus, augite zones in EETA79001B seem to have similar crystallography to those in QUE94201 pyroxene as well as similar composition.

EETA79001A pyroxenes are much smaller in size, but some pyroxenes seem to contain augite mantles. However, it is not clear whether these pyroxenes are typical, and further detailed map analysis is required.

PETROGENETIC RELATION BETWEEN QUE94201 AND LITH. B OF EETA79001

REE studies of QUE94201 suggest that it shows the closest match to EETA79001B [7, 8]. The texture of QUE94201 is also similar to EETA79001B in that both meteorites have abundant large maskelynite. Modal analysis of maskelynite in both QUE94201,34 and EETA79001B (EETA79001,445) gives the same maskelynite abundance, 43%, in both samples. On the other hand, Shergotty and Zagami have smaller amounts of maskelynite (Shergotty: 23%; Zagami: 18%) [9, 10]. Maskelynite of QUE94201 is more coarse-grained than that in EETA79001B, but they are almost comparable. It has been proposed that QUE94201 crystallized from a super-cooled magma [*e.g.*, 4, 5], and plagioclase crystallization played an important role in pyroxene zoning [*e.g*, 1, 3, 4, 5].

The presence of complexly zoned pyroxenes of similar chemical composition both in QUE94201 and EETA79001B indicates that these meteorites followed similar crystallization history that was different from other basalitc shergottites. The high abundance of maskelynite suggests that plagioclase crystallization began during pyroxene growth, possibly from a melt that was supersaturated in plagioclase. However, whitlockite, opaque phases, and mesostatis are more enriched in QUE94201 than EETA79001B, and this shows more evolved nature of QUE94201 [e.g., 1,10]. Although difference is not major, it is suggested that basaltic shergottites can be divided into two sub-groups of maskelynite-poor (Shergotty, Zagami and EETA79001A) and maskelynite-rich (EETA79001B and QUE94201) ones. The sub-grouping of basaltic shergottites are supported from pyroxene mineral zoning as shown in this study.

Acknowledgments: We thank MWG and NIPR for the meteorite samples. Discussion with Prof. H. Takeda of Chiba Inst. Tech. was very much helpful. This work was partially supported by Grant-in-Aid for Encourage. of Young Scientists by the Japanese Ministry of Education (No. 08740410) and Ito Science Foundation.

References: [1] Harvey R. P. *et al.* (1996) *LPSC **XXVII***, 497-498. [2] Kring D. A. *et al.* (1996) *LPSC **XXVII***, 705-706. [3] McKay G. *et al.* (1996) *LPSC **XXVII***, 851-852. [4] McSween H. Y. Jr. and Eisenhour D. D. (1996) *LPSC **XXVII***, 853-854. [5] Mikouchi T. *et al.* (1996) *LPSC **XXVII***, 879-880. [6] Bence A. E. et al. (1971) *Proc. 2nd LSC*, 559-574. [7] Mittlefehldt D. W. and Lindstrom M. M. (1996) *LPSC **XXVII***, 887-888. [8] Dreibus G. *et al.* (1996) *Meteorit. Planet. Sci.*, ***31 (Suppl.)***, A39-A40. [9] Stolper E. and McSween H. Y. Jr. (1979) *GCA*, ***43***, 1475-1498. [10] McCoy T. J. *et al.* (1992) *GCA*, ***56***, 3571-3582.

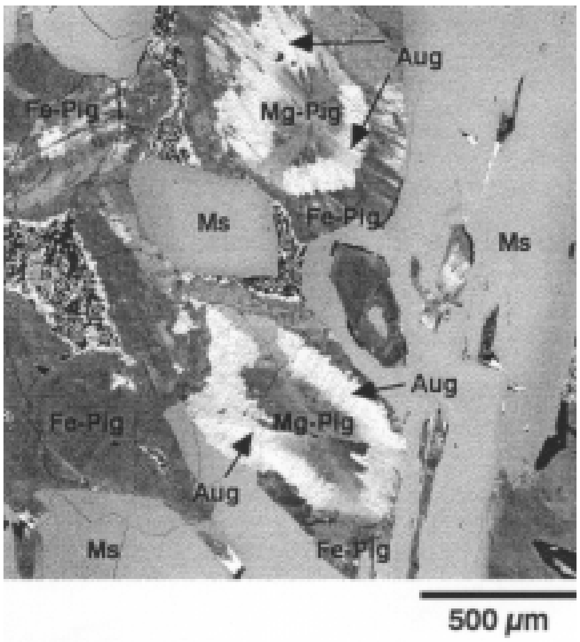

Fig. 1a. Ca X-ray map of QUE94201.

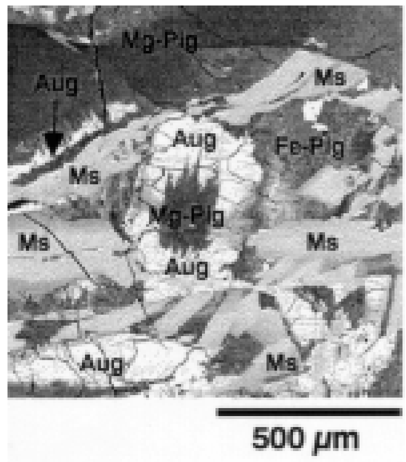

Fig 2a. Ca X-ray map of EETA79001B.

Mg-Pig = Mg-rich pigeonite, Aug = Augite, Fe-Pig = Fe-rich pigeonite, Ms = maskelynite.

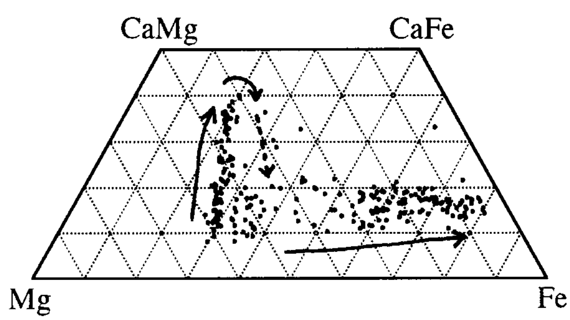

Fig. 1b. QUE94201 pyroxene.

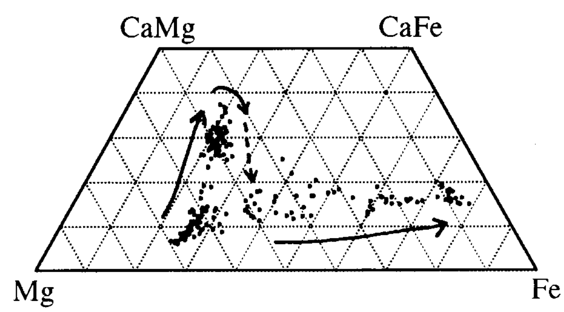

Fig. 2b. EETA79001B pyroxene.